Lecithin as a putative biodegradable blocker of SARS-CoV-2

Muhammad Nawaz Qaisrani[a,b,1]**, Jawad ur Rehman**[c,2]**, Roman Belousov**[a]**, Elham Moharramzadeh Goliaei**[a]**, Ivan Girotto**[a]**, Ricardo Franklin**[a]**, Oriol Güell**[d,*]**, Ali Hassanali**[a,*]**, and Édgar Roldán**[a,*]

[a]ICTP - The Abdus Salam International Centre for Theoretical Physics, Strada Costiera 11, 34151 Trieste, Italy; [b]SISSA - International School for Advanced Studies, Via Bonomea 265, 34136 Trieste, Italy; [c]University di Trieste; [d]Comercial Douma S.L., Carrer de València 5, 08015 Barcelona, Spain

Understanding the physical and chemical properties of viral infection at molecular scales is a major challenge of the scientific community in the fight against the Coronavirus (COVID-19) pandemic. We employ all-atoms molecular dynamics simulations to study the interaction between the receptor-binding domain (RBD) of the SARS-CoV-2 spike protein and the surfactant lecithin, in water solutions. Our microsecond simulations reveal a preferential binding of lecithin to the receptor-binding motif (RBM) of SARS-CoV-2. Furthermore, we find that the lecitin-RBM binding events are mainly dominated by the hydrophobic interactions, which are accompanied by dewetting of water molecules near the RBM. These proof-of-concept simulations provide a demonstration of the use of biodegradable phospholipids as blockers of binding of SARS-CoV-2 with the human Angiotensin Converting Enzyme 2 (ACE2) receptor.

SARS-CoV-2 | Coronavirus | COVID-19 | Spike protein | Lecithin | Molecular dynamics

O ver the last century, humanity has been threatened by several deadly viruses including Spanish flu, SARS Coronavirus (SARS-CoV), Influenza A (H1N1, H5N1), Ebola, Middle East Respiratory Syndrome (MERS-CoV), Zika, and recently Coronavirus disease 2019 (COVID-19 or SARS-CoV-2) [1–3]. To date, the total number of COVID-19 positive cases are in the order of millions according to the World Health Organization report [4]. Due its rapid transmission and high rate of mortality, scientists from different disciplines are putting together efforts in the global endeavour of tackling the Coronavirus pandemic.

The molecular structure of SARS-CoV-2 is formed by lipid membrane, nucleocapsid proteins, and spike proteins, which together shield the RNA genome of the virus. It has been shown that spike proteins play a key role in virus fusion and entry [5], hence they have become one of the key targets for drug design and vaccine development [6–9]. SARS-CoV-2 spike protein is formed by two subunits, denoted by S1 and S2. The S1 subunit binds through its receptor bonding motif (RBM) to the ACE2 (Angiotensin-converting enzyme 2) on the cell membrane surface of lung. On the other hand, the S2 subunit mediates the fusion of the virus with the human host cells [10]. In addition, it is believed that variations in S and ACE2 sequences can not allow for viral infection across species [11, 12]. Recent work has shown that SARS-CoV-2 spike protein binds to ACE2 human receptor with approximately 15nM affinity which is higher than the affinity of SARS-CoV S to ACE2 [13] and it leads to increase virulence of COVID-19 [11, 14, 15]. The protein and ACE2 can interact via hydrogen bonding, hydrophobic and electrostatic interactions [16–18]. There have been numerous attempts to design or re-purpose drugs that would inhibit the binding of the spike protein to ACE2 [19–22]. However, the underlying physical principles that drive these interactions are yet poorly understood. To explore novel and potent drugs, a fundamental understanding of the interplay of molecular forces involving the spike protein, potential inhibitors and of course the surrounding aqueous medium, is critical.

Herein we adopt an unorthodox yet holistic approach and focus our efforts on proof-of-concept simulations that demonstrate that the binding sites of SARS-CoV-2 with ACE2 can be blocked by "soapy" molecules. Specifically, we show with microsecond timescale atomistic molecular dynamics simulations, that a bio-degradable, amphiphilic molecule, phosphatidylcholine (POPC) which forms the phospholipid constituent of a commercially well-known product called lecithin. We show that his molecule appears to form strong and stable aggregates driven by hydrophobic interactions and water dewetting, in close proximity to the RBM zone and may thus hinder interactions with the ACE2 receptor.

The role of water and hydrophobicity in viral inhibition is not unprecedented. Specifically, recent works have reported the efficiency of CB6 antibody and EK1C4 inhibitor in building hydrophobic interactions with SARS-CoV-2 [23, 24]. On the other hand, B38 antibody binds to SARS-CoV-2 RBM via hydrophilic interactions, proposing that water molecules play an important role in the interaction [25]. Interestingly, the role of hydrophobicity and hydrogen bond networks have also been implicated in the interactions of both Zika and HIV viral membranes constituted by POPC bilayers [26, 27].

In the following we study, using molecular dynamics simulations, the interaction between SARS-CoV-2 receptor binding domain (RBD) and a biodegradable molecule that can be extracted from both vegetable oils (e.g. soybean) and animal tissues (e.g. eggs) [28, 29]. More precisely, we focus on the phosphatidylcholine called 1-palmitoyl-2-oleoyl-sn-glycero-3-phosphocholine $C_{42}H_{82}NO_8P$ (POPC), which we will refer to throughout the paper as lecithin. We show that this molecule binds preferentially the receptor binding motif (RBM) of the spike protein driven by the formation of non-polar contacts. Furthermore, lecithin significantly alters the secondary structure of the spike protein to an extent that is strongly modulated by the concentration of the phospholipid. Notably, all these processes are accompanied by a significant change in the water fluctuations at the vicinity of the RBM interface. These results
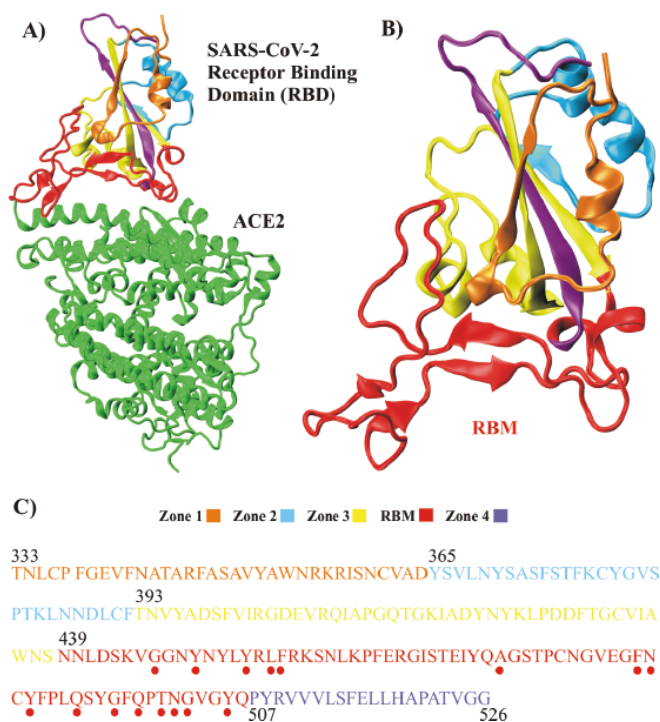
Fig. 1. A) Illustration of the X-ray crystal structure of SARS-CoV2 spike protein receptor binding domain (RBD, multicolor) and human ACE2 receptor (green) (31). **B)** Zoomed view of SARS-CoV-2 RBD, where different colours indicate different zones selected to interrogate the RBD-lecithin interactions at different solvent exposures. The red highlighted part is the receptor-binding motif (RBM) of the protein. **C)** Amino acid sequence corresponding to the crystal structure of SARS-CoV-2 RBD with the different zones highlighted in different colors. The red dots below few residues indicate those amino acids involved in the interaction with the human ACE2 receptor.

open up the possibility of the use of surfactants in drug design.

1. System Setup

In this section we introduce and discuss physicochemical properties of the system in which we focus our study, the SARS-CoV-2 receptor binding domain (RBD) and lecithin in water.

A. SARS-CoV-2 receptor binding domain. Figure 1A illustrates the crystal structure of SARS-CoV2 RBD (multi-colour) bound to the human ACE2 receptor (green)(30). A zoomed-in view of the RBD crystal structure is displayed in Fig. 1B with the RBM highlighted in red. The residue sequence and its cryo-EM structure of S glycoprotein's RBD were adopted from Ref. (30). In order to dissect, and better interrogate the protein-lecithin interactions we divided the RBD into non-overlapping zones. Fig. 1B shows the five different regions in different colors in the protein structure labelled as Zone 1 (orange), Zone 2 (cyan), Zone 3 (yellow), the receptor-binding motif RBM (red) and Zone 4 (purple). The RBM is the largest domain and carries the residue sequence from Asn439 to Gln505 which has been shown to interact with human ACE2 receptor (31).

B. Lecithin. While it is well known that surfactant-protein interactions play an important role in biological contexts, the underlying physical driving forces that drive these processes remain poorly understood(32). Here, we focus our efforts

on the phospholipid POPC (1-palmitoyl-2-oleoyl-sn-glycero-3-phosphocholine), which we will refer throughout the paper as lecithin, a biodegradable, essential phospholipid for the human body. Lecithins are ubiquitous in mammalians organs, they help to build the largest choline reservoir and they are found in the bile (33), and more importantly in the alveolar surface in the lung (34, 35). Lecithin's chemical structure is shown in Fig. 2A. It is a surfactant consisting of a glycerol backbone sterified in positions 1 and 2 with a palmitic and an oleic acid, both constituting the hydrophobic non-polar tail able to interact with non-polar residues. The position 3 of the backbone is linked to a phosphate group which is bonded to a choline group, forming the hydrophilic polar head of lecithin.

Lecithin is amphiphilic and therefore has potential to interact with the spike protein using a combination of both polar and non-polar interactions. In fact, the hydrophilic-lipophylic balance (HLB) of lecithin ranges from values to 4 ± 1 to 9.7 ± 1 (36). Thus, it lies in the range of w/o (water in oil) emulsifying agents and also of wetting spreading agents. This is a crucial property that makes lecithin POPC an ideal candidate to act as a molecule targeting SARS-CoV-2, since one will need both polar and non-polar parts, the former related to the polar amino acids of proteins, whereas the latter involves the protein hydrophobic regions. Moreover, at large concentrations lecithin can aggregate into micelles (37). As we will see later, the aggregation of lecithin in close proximity to the spike protein might serve as a blocking mechanism for ACE2 binding with SARS-CoV-2.

2. Results

We performed all-atoms molecular dynamics (MD) simulations using the open-source software GROMACS 2020 (38, 39). All our simulations were conducted in the canonical NVT ensemble at a temperature of $T = 298.5$K, within a cubic simulation box with side-length 10nm and periodic boundary conditions containing 30634 water molecules. A time step of 2fs was used for all simulations. To simulate the interaction between SARS-CoV-2 RBM, lecithin and water, we employed the OPLS-AA (40) force field together with the SPC/E model of water (41). After an initial equilibration of the RBD crystal structure for ~2 ns, we ran production simulations of 1.2 μs long. In order to assess the role of increasing concentration of lecithin, four different values of lecithin concentration, corresponding to $N_L = 0$ (RBD + water), 5 (RBD + lecithin + water), 10 and 15 lecithin molecules in the simulation box, were used. For each simulation containing lecithin, three independent initial conditions were launched. See computational Methods A for further details.

In order to build our intuition on the nature of the interactions between lecithin and the spike protein, we begin by inspecting representative snapshots of our molecular dynamics simulations (see Supplementary Movies **??**). Figure 2B shows the initial condition in a zoomed-in snapshot of the simulation box for $N_L = 10$ lecithin molecules. Over time, lecithin molecules −initially at random positions in the simulation box− diffuse into the hydration shell of the protein and appear to have an affinity for certain regions of the spike protein. More specifically, we observe that lecithin molecules adhere to the RBM zone as well as Zone 2. Figures 2C-D are representative snapshots taken after $1\mu s$ simulation time for lecithin concentrations corresponding to $N_L = 10$ and
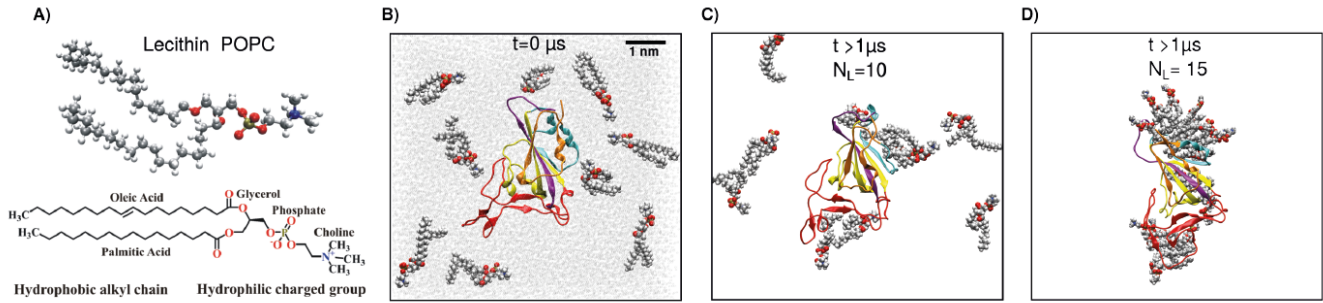
Fig. 2. A) Molecular (top) and chemical (bottom) structure of a lecithin POPC (1-palmitoyl-2-oleoyl-sn-glycero-3-phosphocholine) molecule. The bottom figure highlights its polar (hydrophilic) and non-polar (hydrophobic) chemical groups. **B)** Snapshot of the one initial condition of the simulation setup at, showing the receptor binding domain of SARS-CoV-2 spike protein in the lecithin solution, with water molecules depicted as transparent gray spheres. **C-D)** Snapshots taken at times larger than $1\mu s$ for two different values of the lecithin concentrations corresponding to 10 (C) and 15 (D) number of lecithin molecules in the simulation box. For the sake of better visualization, we do not include the water molecules in panels C and D.

$N_L = 15$ illustrating this phenomenon.

There are several interesting features that one can observe in these binding events of involving lecithin. Firstly, lecithin molecules stick around the RBM and Zone 2 either as single molecules (Fig. 2C) or in the form of clusters (Fig. 2D). Furthermore, the simulations also reveal that lecithin docks to the viral protein mostly involving the hydrophobic non-polar tail. Overall, Figure 2D shows the aggregation of lecithin into two clusters, one near the RBM and another in close proximity to Zone 2 (cf. Fig. 1B). Note that Zone 2 is exposed to the solvent in our simulations, but is bound to the core of the spike protein in the virus, hence it may be accessible to lecithin when the spike-protein trimer opens due to fluctuations or interactions with other proteins.

In the following, we provide a quantitative analysis of our simulations, by first looking in Sec. 2A at the global structural behavior of the SARS-CoV-2 RBD monitoring its radius of gyration. To investigate the protein-lecithin interactions at the atomic level, we present in Sec. 2B a detailed contact map analysis disentangling the interactions involving the polar and non-polar groups of the lecithin molecules with different SARS-CoV-2 RBD residues. As we will see later, in Sec. 2C, the interaction of the hydrophobic parts of lecithin with the spike protein, reveals the crucial role of water fluctuations during the interaction of the spike protein with its aqueous environment.

A. Radius of Gyration. To monitor the change in the structure of SARS-CoV-2 RBD resulting from its interaction with lecithin, we measure the radius of gyration (RG) of the RBD as a function of time. In particular, we evaluate $\mathrm{RG}(t) = \left(\sum_i m_i ||\mathbf{r}_i(t)||^2 / \sum_i m_i \right)^{1/2}$, where m_i and $\mathbf{r}_i(t)$ is the mass and position of each i-th atom respectively, with respect to the center of mass of the molecule to which it belongs to. We consider here two different RGs of interest: (i) RG of all the heavy atoms in the SARS-CoV-2 RBD; and (ii) RG of all the heavy atoms in the RBM. The distribution of the RGs (Figs. 3A-B) show that lecithin significantly changes the structure of the RBD and in particular, the RBM part and that this effect is highly sensitive to the concentration of lecithin in water.

B. Atlas of Lecithin-Spike Protein Molecular Interactions. In this section, we investigate the interatomic contacts that form
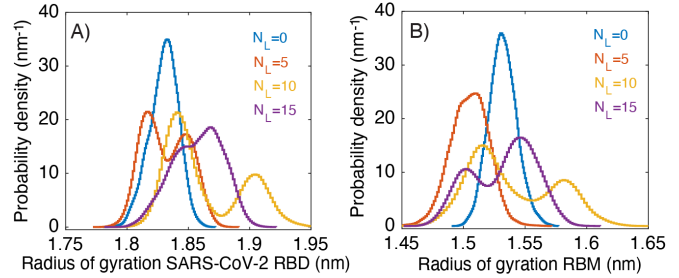

Fig. 3. Distribution of radius of gyration of SARS-CoV-2 spike protein receptor binding domain RBD **(A)** and of its receptor binding motif RBM **(B)** for different concentrations of lecithin (see legend, where N_L denotes the number of lecithin molecules). The data is obtained from a single $1\mu s$ molecular-dynamics simulation for each lecithin concentration value.

between lecithin and spike protein. To this aim, we plot in Fig. 4 contact maps between all the heavy atoms [*] in the protein residues of SARS-CoV-2 RBD and lecithin molecules for the lecithin concentration value $N_L = 15$. We focus this analysis on two quantities, namely the average interatomic distance (Fig. 4A-B) and the average interaction time (Fig. 4C-D) between lecithin and the different viral protein zones (see Fig. 1). Figs. 4A and C, show the interaction distances and times that lecithin forms with the entire RBD. Consistent with Fig. 2, we observe that there are some hot-spot regions where lecithin prefers to bind, in particular, Zone2 and RBM. Within these regions, the interatomic distances between lecithin and the viral protein are less than one nanometer. Since the RBM zone is the one that interacts with ACE2 we focus on examining its contacts with lecithin in Fig. 4B. Specifically, lecithin appears to form close contacts with amino acids 473-490, which contain ACE2-interacting residues (cf. Fig. 1C).

The bottom panels of Fig. 4 show the corresponding maps built on the interaction times associated with lecithin and the protein. In order to classify the times of interaction, a threshold distance of 1nm corresponding to the typical range of van-der-Waals forces, was used. We find that the average interaction time between lecithin and the RBD is on the order of hundreds of nanoseconds. As expected, the core of the protein (Zone 3) is characterized by the weakest binding. We observe

---

[*] All our contact maps are evaluated taking into account the positions of all except the hydrogen atoms, i.e. only the *heavy* atoms.
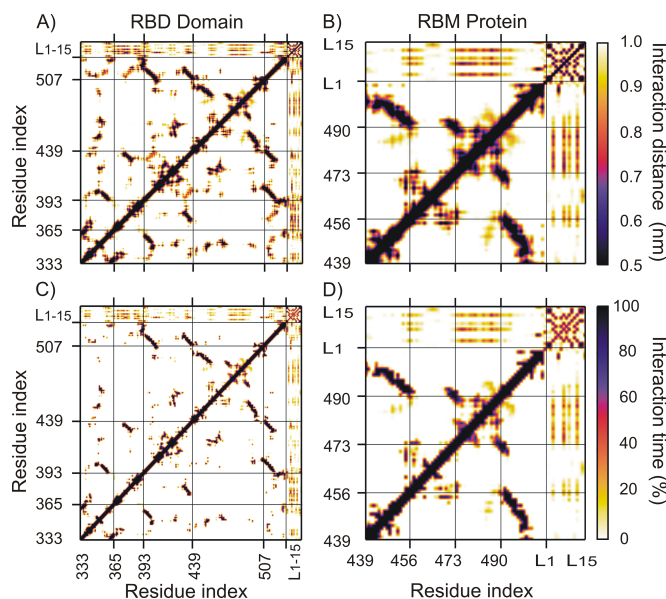
Fig. 4. A) Contact map between different zones of SARS-CoV-2 receptor binding domain (RBD) and lecithin molecules. The positions of all the heavy atoms are used to define contacts as function of distances up to 1nm scale (see colorbar). **B)** Zoomed-in view of (A) showing the interaction distance contact map between the RBM zone and lecithin molecules. **C-D)** Total interaction time (relative to the simulation time, in %) of lecithin molecules with SARS-CoV-2 RBD **(C)** and with its RBM **(D)**. The latter is given by the time spent at distances below 1nm.

Fig. 5. Average contact maps between different zones of SARS-CoV-2 receptor binding domain (RBD) and lecithin polar **(A)** and non polar **(A)** groups, see text for more details.

similar trends in our simulations at lower concentrations of lecithin, i.e for $N_L = 5$ and $N_L = 10$ lecithin molecules (see the SI).

To gain further insights into the physical driving force between the molecular interactions, we investigate the average contact maps of polar and non polar groups of lecithin molecules with the RBM residues. To this aim, we compute the average interatomic distance between the RBM atoms and two different parts of lecithin molecules: (i) the hydrophobic alkyl chain (see Fig. 5B); and (ii) the hydrophilic charged group (see Fig. 5C). Notably, the interatomic distance between all the subdomains of the RBM and the hydrophobic tail of lecithin molecules is significantly smaller than the distance to the hydrophilic head. Therefore the lecithin-RBM contacts are mainly dominated by the hydrophobic interactions and in fact, this is enhanced under higher concentrations of lecithin.

C. Water dewetting near the receptor-binding motif. It is well known that water plays an instrumental role in tuning the structural and dynamical properties of biological systems (42). In the context of our work, there have been numerous studies showing the important role of water dewetting in facilitating the hydrophobic interactions proteins (43, 44). The preceding analysis, shows that hydrophobic interactions between the non-polar groups of lecithin form close contacts with the RBM. In order to explore the importance of the reorganization of the solvent environment during the RBM-lecithin binding, we show in Fig. 6 the radial distribution of water molecules $g(r)$ of sixteen residues in the RBM, which have been implicated in the docking mechanism of SARS-CoV-2 and ACE2 (45).

In order to probe the dewetting of the RBM's surface induced by the presence of lecithin in the water solution, we illustrate the RDFs of two amino acids, Ala475 and Phe486
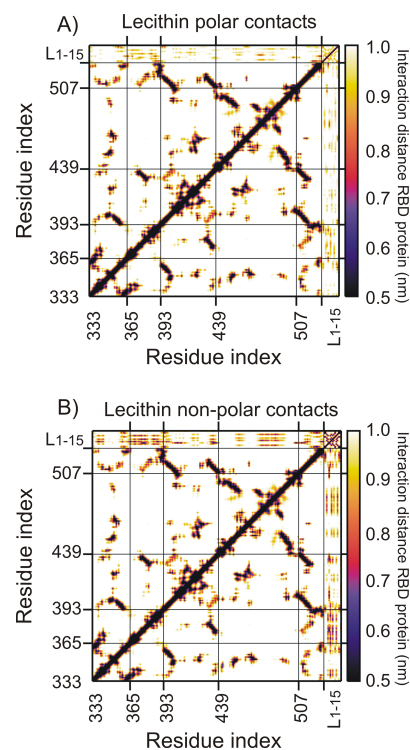
which correspond to alanine and phenylalanine both of which are hydrophobic residues (dashed curves correspond to RBM in the absence of lecithin and solid with $N_L = 15$). Strikingly, we observe that there is a drastic depletion in the water density over a length scale of 1nm near both these amino acids in the presence of lecithin. This effect can be clearly seen in Fig. 7 which illustrates the hydration shell around Phe486 in the absence and in the presence of a cluster of lecithin.

The RBM zone interacting with ACE2 is actually made up of sixteen amino acids. In order to establish how the solvent reorganizes across the entire RBM-ACE2 binding region, we determined the hydration shell outer radius r_o, defined as the position of the Gibbs dividing interface, for these sixteen aminoacids with and without lecithin in solution. Notably, r_o increases upon addition of lecithin for all these residues. The inset of Fig. 6 shows the relative change of the sixteen amino acids r_o in the RBM-ACE2 junction. All sixteen undergo a depletion of water density to different extents, with residues Ala475 and Phe486 displaying a striking increase of more than 100%.

3. Discussion

In this work we have studied with molecular dynamics simulations the interaction between SARS-CoV-2 receptor binding domain (RBD) and lecithin molecules in water. Our main results are summarized as follows: (i) lecithin induces a conformational change in the RBD and its receptor binding motif which is revealed by an increase of the radius of gyration with the lecithin concentration; (ii) lecithin molecules bind mostly by docking their hydrophobic tails into the viral protein surface. This hydrophobic interaction occurs at distances that are
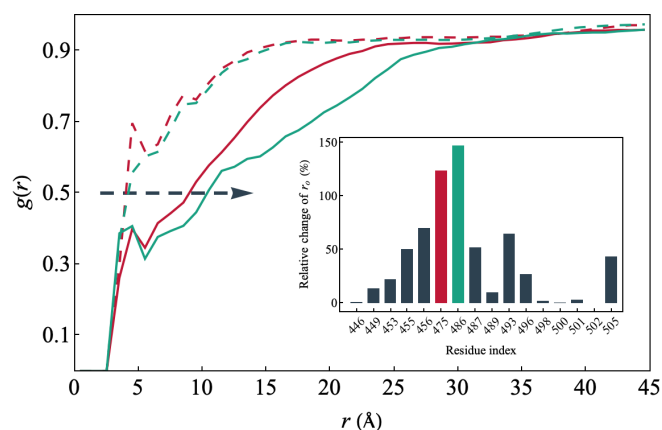
Fig. 6. Radial distribution function $g(r)$ of water molecules plotted as a function of distance r from the 16 amino acids of the RBM domain which are involve in binding with ACE2 (the residues highlighted with red dots in panel C) of Fig. 1). The analysis is done for 1.2 μs long trajectory of system with $N_L = 15$ (solid lines) and $N_L = 0$ (dashed lines) lecithin in water solution respectively. The horizontal line illustrates the increase of the hydration shell's outer radius r_o, which is delimited by the position of the Gibbs dividing interface $g(r_o) = 0.5$. We reproduce $g(r)$ only for the amino acids Ala475 and Phe486, near which the hydration shell is depleted the most due to the hydrophobic interactions with the lecithin molecules. The inset reports the percentage change of r_o for all the sixteen residues that we examined. Ala475 and Phe486 are singled out by the same colors as in the main plot. Note that as reference positions of the H_2O groups and amino acids we chose the oxygen and the alpha carbon atoms, respectively.

₂₈₈ smaller than 1nm and on timescales on the order of ~ 100ns. ₂₈₉ (iii) The lecithin-RBD hydrophobic binding is accompanied by ₂₉₀ a dewetting of water molecules in the receptor binding motif. ₂₉₁ Taken all together, these results suggest the possible role of ₂₉₂ soapy-like molecules as potential biodegradable blockers of the ₂₉₃ interaction between SARS-CoV-2 RBD and ACE2 receptor.

₂₉₄ As stressed earlier, the observations we make here of lecithin ₂₉₅ SARS-CoV-2 interactions serves as a proof of concept for the ₂₉₆ role of surfactants in drug design. For example, phospholipids ₂₉₇ have been employed earlier to treat SARS-CoV [46]. Moreover, ₂₉₈ lecithin has been used as drug component to dose lactoferrin ₂₉₉ for SARS-CoV-2 prevention [47]. Finally, a key point of our ₃₀₀ study is that the presented results could be extended to a ₃₀₁ mixture of amphiphilic phospholipids, not only limited to ₃₀₂ lecithin.

₃₀₃ While we cannot make any quantitative predictions on the ₃₀₄ binding affinities or kinetics from our current simulations, the ₃₀₅ insights we have uncovered involving the important role of ₃₀₆ hydrophobic interactions and water fluctuations, is an impor- ₃₀₇ tant result. In a time where a microscopic understanding of ₃₀₈ this global pandemic remains unknown, we believe that these ₃₀₉ simulations make important first steps to fill this gap.

ACKNOWLEDGMENTS

Supporting Information Appendix (SI).

A. Computational Methods. To investigate the structural and dynamical behaviour of SARS-COV2 RBD protein in clean water and concentrated POPC solutions, all atoms molecular dynamics (MD) simulations were conducted using the
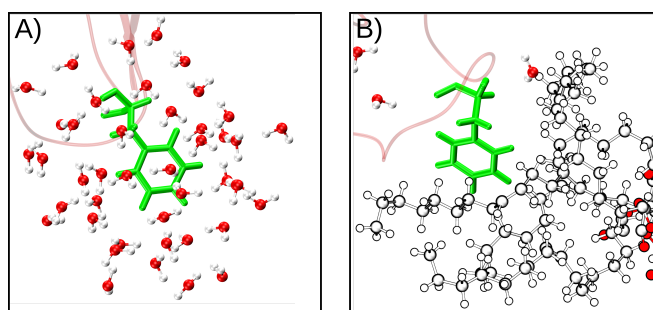

Fig. 7. A) Zoomed Snapshot taken from the simulation of the system where protein is in pure water and B) when protein is in lecithin solution. The hydration water within 5 Å from the Phe486 residue (in green) which is the part of RBM (transparent red coils) is shown in both cases. In the vicinity of lecithin cluster (shown by glassy balls and sticks) when it formed near the RBM residues over hundreds of nanoseconds simulation time, the hydration shell is significantly depleted due to the hydrophobic interaction of lecithin molecules hence dewetting of the protein residues.

multi-GPUs version of the open-source package GROMACS 2020 [38, 39]. Adopting an high-throughput approach we ran multiple simulations in parallel on several compute nodes of the recently installed Marconi100 at CINECA, a world-class European Tier-0 system for high-performance computing (HPC). ach simulation was performed with the single node version (threadMPI+CUDA) of the software, highly optimized to fully exploit the compute capability available on the accelerated cluster. Indeed, a single compute node of Marconi100 is equipped with 2x IBM Power9 CPUs and 4x V100 NVIDIA GPUs, delivering high-bandwidth data streaming between the CPUs and GPUs via NVLink 2.0. In particular, three of the GPUs on the Marconi100's nodes were used for computing the particle-particle force interaction, while having one GPU dediacted to compute the PME long-range electrostatic calculations, in a configuration capable to deliver a performance up to about 190ns/day of MD simulation, using a single compute node of the accelerated system for HPC. In all these simulations, we used the OPLS-AA[40] force field together with the SPC/E water model(). The dimensions of the simulation box were 10 nm in the cubic geometry, containing 30634 water molecules. The simulations with concentrated lecithin solution were performed using number of lecithin molecules $N_L = 5$, $N_L = 10$, $N_L = 15$ respectively. Furthermore, to assess the sensitivity of different choices of the POPC molecules positions at $t = 0$ in the simulation box, three different initial conditions were generated for each concentration of the lecithin solution. A cut-off radius of 1.2 nm was used to create a non-bonded pair list. For the short-range non-bonded interactions a cut-off length at 1.1 nm was chosen for a shifted Lennard-Jones potential while the long-range electrostatic interactions were taken into account via Particle Mesh Ewald-Switch[48] (PME-switch) method with a Coulomb switching cut-off at 1.2 nm. A long-range dispersion correction was applied for truncating the van-der-Waals interactions. All bonds were constrained using the LINCS algorithm[49]. A time step of 2 fs was used for the Verlet integrator. All simulations were conducted in the canonical ensemble (NVT) at 298.5 K using the velocity-rescale thermostat[50] with a time-constant of 0.1 ps. The production runs for all simulations after initial equilibration were extended up to 1.2 μs.

References

1. LC McDonald, et al., Sars in healthcare facilities, toronto and taiwan. *Emerg. infectious diseases* **10**, 777 (2004).
2. SY Cho, et al., Mers-cov outbreak following a single patient exposure in an emergency room in south korea: an epidemiological outbreak study. *The Lancet* **388**, 994–1001 (2016).
3. LA Reperant, AD Osterhaus, Aids, avian flu, sars, mers, ebola, zika... what next? *Vaccine* **35**, 4470–4474 (2017).
4. World health organization. coronavirus disease 2019 (covid-19)-situation report-146 (2020).
5. N Wang, J Shang, S Jiang, L Du, Subunit vaccines against emerging pathogenic human coronaviruses. *Front. microbiology* **11**, 298 (2020).
6. J Cohen, Vaccine designers take first shots at covid-19 (2020).
7. TM Abd El-Aziz, JD Stockand, Recent progress and challenges in drug development against covid-19 coronavirus (sars-cov-2)-an update on the status. *Infect. Genet. Evol.* **83**, 104327 (2020).
8. L Peeples, News feature: Avoiding pitfalls in the pursuit of a covid-19 vaccine. *Proc. Natl. Acad. Sci.* **117**, 8218–8221 (2020).
9. N Vankadari, Arbidol: A potential antiviral drug for the treatment of sars-cov-2 by blocking the trimerization of viral spike glycoprotein? *Int. J. Antimicrob. Agents*, 105998 (2020).
10. P Zhou, et al., A pneumonia outbreak associated with a new coronavirus of probable bat origin. *nature* **579**, 270–273 (2020).
11. Y Wan, J Shang, R Graham, RS Baric, F Li, Receptor recognition by the novel coronavirus from wuhan: an analysis based on decade-long structural studies of sars coronavirus. *J. virology* **94**, 1–9 (2020).
12. Z Liu, et al., Composition and divergence of coronavirus spike proteins and host ace2 receptors predict potential intermediate hosts of sars-cov-2. *J. medical virology* **92**, 595–601 (2020).
13. D Wrapp, et al., Cryo-em structure of the 2019-ncov spike in the prefusion conformation. *Science* **367**, 1260–1263 (2020).
14. AC Walls, et al., Structure, function, and antigenicity of the sars-cov-2 spike glycoprotein. *Cell* **181**, 281–292 (2020).
15. R Yan, et al., Structural basis for the recognition of sars-cov-2 by full-length human ace2. *Science* **367**, 1444–1448 (2020).
16. A Choudhury, S Mukherjee, In silico studies on the comparative characterization of the interactions of sars-cov-2 spike glycoprotein with ace-2 receptor homologs and human tlrs. *J. medical virology*, 1–9 (2020).
17. Y Wang, M Liu, J Gao, Enhanced receptor binding of sars-cov-2 through networks of hydrogen-bonding and hydrophobic interactions. *Proc. Natl. Acad. Sci.* **117**, 13967–13974 (2020).
18. M Amin, MK Sorour, A Kasry, Comparing the binding interactions in the receptor binding domains of sars-cov-2 and sars-cov. *The J. Phys. Chem. Lett.* **11**, 4897—-4900 (2020).
19. V Monteil, et al., Inhibition of sars-cov-2 infections in engineered human tissues using clinical-grade soluble human ace2. *Cell* **181**, 905–913 (2020).
20. H Zhang, JM Penninger, Y Li, N Zhong, AS Slutsky, Angiotensin-converting enzyme 2 (ace2) as a sars-cov-2 receptor: molecular mechanisms and potential therapeutic target. *Intensive care medicine* **46**, 586–590 (2020).
21. Y Han, P Král, Computational design of ace2-based peptide inhibitors of sars-cov-2. *ACS nano* **14**, 5143–5147 (2020).
22. B Nami, A Ghanaeian, K Ghanaeian, N Nami, The effect of ace2 inhibitor mln-4760 on the interaction of sars-cov-2 spike protein with human ace2: a molecular dynamics study. (2020).
23. R Shi, et al., A human neutralizing antibody targets the receptor binding site of sars-cov-2. *Nature*, 1–8 (2020).
24. S Xia, et al., Inhibition of sars-cov-2 (previously 2019-ncov) infection by a highly potent pan-coronavirus fusion inhibitor targeting its spike protein that harbors a high capacity to mediate membrane fusion. *Cell research* **30**, 343–355 (2020).
25. Y Wu, et al., A noncompeting pair of human neutralizing antibodies block covid-19 virus binding to its receptor ace2. *Science* **368**, 1274–1278 (2020).
26. J Sun, Y Li, P Liu, J Lin, Study of the mechanism of protonated histidine-induced conformational changes in the zika virus dimeric envelope protein using accelerated molecular dynamic simulations. *J. Mol. Graph. Model.* **74**, 203–214 (2017).
27. G Meher, S Sinha, GP Pattnaik, S Ghosh Dastidar, H Chakraborty, Cholesterol modulates membrane properties and the interaction of gp41 fusion peptide to promote membrane fusion. *The J. Phys. Chem. B* **123**, 7113–7122 (2019).
28. , *Lecithin*. (American Cancer Society), (2006).
29. E Nyankson, MJ DeCuir, RB Gupta, Soybean lecithin as a dispersant for crude oil spills. *ACS Sustain. Chem. & Eng.* **3**, 920–931 (2015).
30. A Spinello, A Saltalamacchia, A Magistrato, Is the rigidity of sars-cov-2 spike receptor-binding motif the hallmark for its enhanced infectivity? insights from all-atoms simulations. *The J. Phys. Chem. Lett.* **11**, 4785—-4790 (2020).
31. J Lan, et al., Structure of the sars-cov-2 spike receptor-binding domain bound to the ace2 receptor. *Nature* **581**, 1–6 (2020).
32. D Otzen, Protein–surfactant interactions: a tale of many states. *Biochimica et Biophys. Acta (BBA)-Proteins Proteomics* **1814**, 562–591 (2011).
33. DM Small, M Bourgès, D Dervichian, Ternary and quaternary aqueous systems containing bile salt, lecithin and cholesterol. *Nature* **211**, 816–818 (1966).
34. M Abrams, Isolation and quantitative estimation of pulmonary surface-active lipoprotein. *J. applied physiology* **21**, 718–720 (1966).
35. D Tierney, J Clements, H Trahan, Rates of replacement of lecithins and alveolar instability in rat lungs. *Am. J. Physiol. Content* **213**, 671–676 (1967).
36. P van Hoogevest, Review–an update on the use of oral phospholipid excipients. *Eur. J. Pharm. Sci.* **108**, 1–12 (2017).
37. RE Ostlund Jr, CA Spilburg, WF Stenson, Sitostanol administered in lecithin micelles potently reduces cholesterol absorption in humans. *The Am. journal clinical nutrition* **70**, 826–831 (1999).
38. MJ Abraham, et al., Gromacs: High performance molecular simulations through multi-level parallelism from laptops to supercomputers. *SoftwareX* **1**, 19–25 (2015).
39. E Lindahl, M Abraham, B Hess, D van der Spoel, the gromacs development team. *GROMACS 2020 Source code (Version 2020). Zenodo.* (2020).
40. WL Jorgensen, DS Maxwell, J Tirado-Rives, Development and testing of the opls all-atom force field on conformational energetics and properties of organic liquids. *J. Am. Chem. Soc.* **118**, 11225–11236 (1996).
41. H Berendsen, J Grigera, T Straatsma, The missing term in effective pair potentials. *J. Phys. Chem.* **91**, 6269–6271 (1987).
42. MC Bellissent-Funel, et al., Water determines the structure and dynamics of proteins. *Chem. Rev.* **116**, 7673–7697 (2016).
43. BJ Berne, JD Weeks, R Zhou, Dewetting and Hydrophobic Interaction in Physical and Biological Systems. *Annu. Rev. Phys. Chem.* **60**, 85–103 (2009).
44. D Chandler, Hydrophobicity: Two faces of water. *Nature* **417**, 491–491 (2002).
45. J Lan, et al., Structure of the sars-cov-2 spike receptor-binding domain bound to the ace2 receptor. *Nature* **581**, 215–220 (2020).
46. R Fleming, Phospholipids for the treatment of infection by togaviruses, herpes viruses and coronaviruses (2005) US Patent App. 10/783,927.
47. G Serrano, et al., Liposomal lactoferrin as potential preventative and cure for covid-19. *Int. J. Res. Heal. Sci* **8**, 8–15 (2020).
48. T Darden, D York, L Pedersen, Particle mesh ewald: An n log (n) method for ewald sums in large systems. *The J. chemical physics* **98**, 10089–10092 (1993).
49. B Hess, H Bekker, HJ Berendsen, JG Fraaije, Lincs: a linear constraint solver for molecular simulations. *J. computational chemistry* **18**, 1463–1472 (1997).
50. G Bussi, D Donadio, M Parrinello, Canonical sampling through velocity rescaling. *The J. chemical physics* **126**, 014101 (2007).